Sādhanā Vol. 28, Parts 3 & 4, June/August 2003, pp. 359–382. © Printed in India

Solidification cracking in austenitic stainless steel welds

V SHANKAR, T P S GILL, S L MANNAN and S SUNDARESAN*

Indira Gandhi Centre for Atomic Research, Kalpakkam 603 102, India
*Department of Metallurgical Engineering, Indian Institute of Technology – Madras, Chennai 600 036, India
e-mail: vshank@igcar.ernet.in

Abstract. Solidification cracking is a significant problem during the welding of austenitic stainless steels, particularly in fully austenitic and stabilized compositions. Hot cracking in stainless steel welds is caused by low-melting eutectics containing impurities such as S, P and alloy elements such as Ti, Nb. The WRC-92 diagram can be used as a general guide to maintain a desirable solidification mode during welding. Nitrogen has complex effects on weld-metal microstructure and cracking. In stabilized stainless steels, Ti and Nb react with S, N and C to form low-melting eutectics. Nitrogen picked up during welding significantly enhances cracking, which is reduced by minimizing the ratio of Ti or Nb to that of C and N present. The metallurgical propensity to solidification cracking is determined by elemental segregation, which manifests itself as a brittleness temperature range or BTR, that can be determined using the varestraint test. Total crack length (TCL), used extensively in hot cracking assessment, exhibits greater variability due to extraneous factors as compared to BTR. In austenitic stainless steels, segregation plays an overwhelming role in determining cracking susceptibility.

Keywords. Austenitic stainless steels; solidification cracking; composition effects; varestraint testing.

1. Introduction

Austenitic stainless steels, particularly those that contain no ferrite, are susceptible to hot cracking during welding. Hot cracking or hot tearing has been investigated in castings (Pellini 1952) and welds (Medovar 1954) for several decades. Hot cracking refers to cracking that occurs during welding, casting or hot working at temperatures close to the melting point of the material. The cracking is known to occur both above the liquation temperature – known as supersolidus cracking (Borland 1960) – and in the solid state, called subsolidus cracking. The various types of hot cracks encountered in stainless steel weldments have been classified by Hemsworth *et al* (1969). Supersolidus cracking may manifest as solidification cracking, occurring in the presence of a liquid phase in the fusion zone, or as liquation cracking in the heat-affected zone (HAZ) where it is accompanied by grain-boundary melting. Solidification cracking in the weld metal is considered the most deleterious and is more widely observed than the other types of cracking.

Although much research experience exists on the nature of hot cracking in stainless steels and various measures required for minimising it, complete understanding of the phenomenon is still lacking. Further, new materials are continuously being developed for various applications such as power systems, nuclear, chemical and petrochemical industries, driven by requirements of higher operating temperatures and lifetimes (Maziasz 1989). The material design criteria for these systems may vary from thermal stability, and resistance to enhanced creep under irradiation and corrosion resistance in various media. Thus, these materials may not be designed primarily to be weldable and there is a continuing need to solve welding problems in their fabrication.

Austenitic stainless steels of the AISI 300 series of stainless steels usually solidify during welding as a mixture of austenite and ferrite. The ferrite almost fully transforms to austenite on cooling, but there could be retention of a few percent of δ-ferrite in the weld metal. The association of δ-ferrite with cracking resistance in stainless steel welds is quite old. As early as 1938, Scherer *et al* (1941) filed a patent, which claimed that crack-resistant weld deposits could be produced if the composition is adjusted to result in 5–35% ferrite in the completed weld. Since then, the problem of cracking in the weld metal can be considered as virtually eliminated in cases where ferrite can be retained in the weld. Nevertheless, solidification cracking continues to cause concern in fully austenitic stainless steels, when ferrite is restricted and when composition adjustments during welding are not possible.

The addition of elements like phosphorus and boron can result in improved irradiation stability and creep properties (Maziasz 1989) and a minimum content of phosphorus is specified on this account. However, impurity elements such as sulphur and phosphorus, and minor alloy elements such as boron, silicon, titanium and niobium promote hot cracking, particularly in fully austenitic steels (Hull 1960).

Nitrogen-added stainless steels exhibit several unique characteristics such as superior strength at ambient as well as high temperatures, excellent corrosion resistance in various media and are candidate materials to replace other more expensive materials. Weldability of type 316LN steels has not been fully investigated and the service record of welding consumables is not currently established. Here, the major consideration is the role of nitrogen in the base metal and consumables during welding. Nitrogen has been reported to increase cracking in primary ferritic-solidifying compositions, but in fully austenitic steels a beneficial effect is reported. Effects of nitrogen on microstructure and cracking behaviour appear to be complex and the mechanisms thereof are not completely understood.

Development of reliable testing methods for reproducible quantitative information on hot cracking susceptibility has been continuing since the 1950s. The varestraint test (Savage & Lundin 1965) and its modifications have been used in a large number of studies on hot cracking susceptibility of materials. The varestraint tests provide several quantitative parameters that have been used for weldability comparisons and process and alloy development (Lundin *et al* 1982). The compositional requirements for fabrication and service properties may be in opposition, and optimal levels must be found for satisfactory weldability. Optimisation of composition based on weldability considerations would require standardised tests and assessment criteria to be evolved. The purpose of this review is to examine the current understanding of solidification cracking in austenitic stainless steels with particular emphasis on nitrogen-alloyed and stabilized stainless steels.

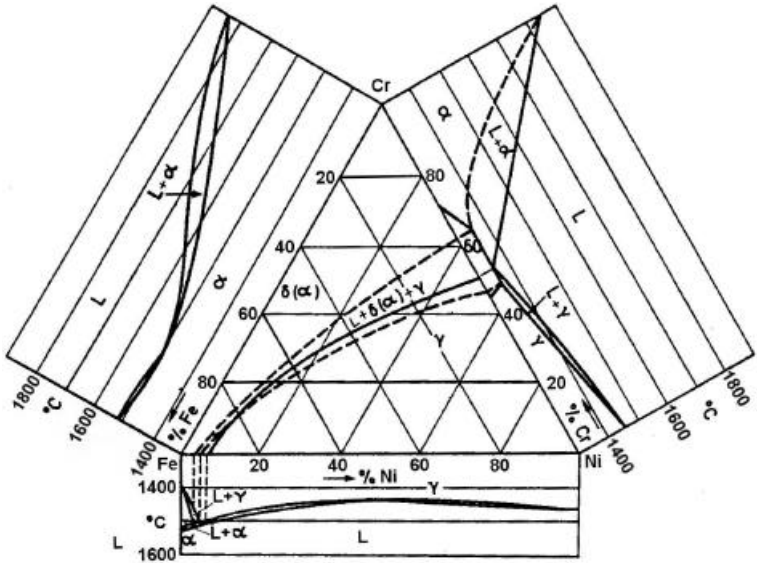

Figure 1. Liquidus and solidus projections of the Fe–Cr–Ni system shown along with the constituent binaries (after Folkhard 1988).

2. Solidification-phase relationships in the Fe–Cr–Ni system

A study of the Fe–Cr–Ni phase diagram is required for an understanding of the solidification behaviour of stainless steel welds. The liquidus and solidus projections of the Fe–Cr–Ni system along with the constituent binaries (Folkhard 1988) are shown in figure 1. The Fe–Cr system is isomorphous down to temperatures well below the solidification range. The Cr–Ni system shows a eutectic at 1618 K (1345° C) and 49 wt.% nickel. In the Fe–Ni system, the δ-ferrite phase on the iron side forms a short peritectic loop, after which the system is completely soluble to 100 wt.% nickel. Thus, in the Fe–Cr–Ni ternary system, the liquidus projection starts at the peritectic reaction on the Fe–Ni system ($\delta + L \leftrightarrow \gamma$) and moves down to the eutectic reaction ($L \leftrightarrow \delta + \gamma$) on the Cr–Ni system. On the Ni- and Cr-enriched side a ternary eutectic is formed at 1573 K (1300°C).

The initial solidifying phase is determined by the position of the alloy with respect to the liquidus surface, which under equilibrium conditions proceeds toward the eutectic/peritectic before solidification is complete. Most stainless steel compositions in wide use occur on the iron-rich side of the ternary between 50 and 70 wt.% iron. The 70 wt.% iron isopleth of the ternary shown in figure 2 is commonly used to identify the primary solidifying phases or solidification modes for various compositions. Four distinct modes are normally considered, viz., austenitic (A), austenitic–ferritic or primary austenitic (AF), ferritic-austenitic or primary ferritic (FA) and ferritic (F). The approximate composition ranges in which these modes occur are indicated in figure 2, while the microstructure and morphology of the phases during and after solidification are shown schematically in figure 3. Alloys solidifying in the A mode will remain unchanged to low temperatures, while those solidifying as AF would form some eutectic ferrite. Compositions that solidify in the FA and F modes pass through the $\delta \leftrightarrow \gamma$ two-phase region and may re-enter the single-phase austenite field. This is due to the asymmetry of the two-phase field towards the primary ferritic side of the diagram, as seen in figure 2. Thus, alloys such as Type 304 and 316 that are fully austenitic at room temperature enter this

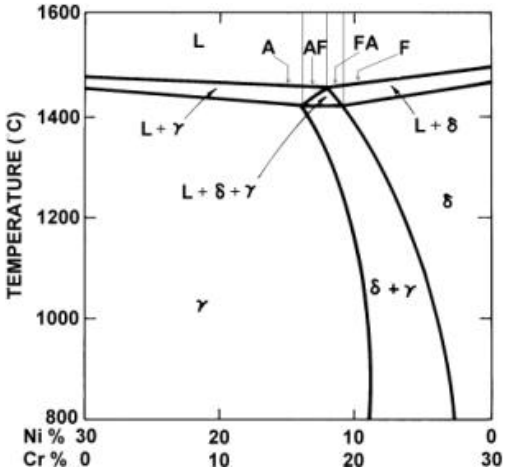

Figure 2. Pseudobinary section of the Fe–Cr–Ni ternary diagram at 70% Fe, showing solidification modes; A - fully austenitic, AF - austenitic–ferritic, FA - ferritic–austenitic and F - fully ferritic.

two-phase region after AF/FA solidification and may undergo solid-state transformation to a fully austenitic structure. For higher ratios of chromium over nickel, the equilibrium structure at room temperature may retain considerable amounts of δ-ferrite as in duplex stainless steels.

The transition from peritectic to eutectic reaction in Fe–Cr–Ni alloys occurs at 17·2 wt.% Cr and 11·9 wt.% Ni (Fredriksson 1979). Under equilibrium conditions, the peritectic reaction occurs only at iron contents above 75 wt.%. However, quenching experiments have revealed that even at higher alloying contents, the peritectic reaction can occur, presumably due to segregation (David *et al* 1979). The solidification in leaner alloys such as Type 304 or 16-8-2 tends to be peritectic while higher alloyed grades undergo eutectic type of reaction. This transition is shifted to lower chromium levels with the addition of molybdenum (Fredriksson 1979). The occurrence of peritectic reaction is important from the point of view of cracking. It is believed that the heterogeneous grain boundaries formed at liquid junctions in peritectic systems retard wetting and crack formation (Matsuda *et al* 1979).

2.1 *Solidification of stainless steel welds*

Under the non-equilibrium solidification conditions prevailing during welding, segregation alters the product phases and their compositions. The segregation of major alloying elements

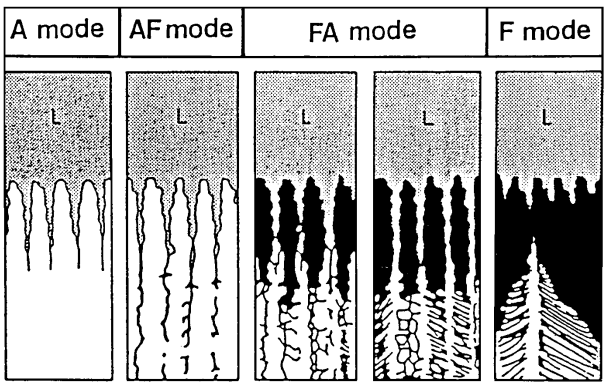

Figure 3. Schematic representation of solidification modes in austenitic stainless steel welds showing phase morphologies (after Koseki & Flemings 1996).

in stainless steel welds has been investigated by Koseki *et al* (1994). In fully austenitic stainless steels, according to them, the interdendritic regions are slightly enriched in both Cr and Ni, while in AF mode weld metal significant enrichment of Cr and depletion of Ni occur in the interdendritic regions. Ferrite nucleates in the Cr-rich and Ni-depleted regions as a non-equilibrium phase. When FA and F mode solidification takes place, the dendrite core is significantly enriched in Cr and depleted in Ni. The segregation of Cr to ferrite and Ni to austenite during solidification plays a major role in stabilizing the ferrite during subsequent solid state transformation.

An important aspect of weld solidification is the effect of solidification kinetics on the phases formed. The eutectic reaction $L \leftrightarrow \delta + \gamma$ in stainless steels is not typical of the classical eutectic in the sense that the composition difference between δ and γ phases is minor. The relatively minor difference in thermodynamic stability of the two phases in the vicinity of the eutectic permits non-equilibrium solidification to a metastable phase obtained by extrapolation of the equilibrium phase boundaries (Kelly *et al* 1984). Thus, the weld microstructure in stainless steels depends significantly on kinetic factors such as cooling rate and epitaxy, apart from equilibirum stability considerations. Under the rapid cooling and fast growth rates aided by epitaxy, the weld structure could solidify far away from equilibrium Bhadeshia *et al* (1991).

In FA or F mode weld metals, 70–100% δ-ferrite may be formed at the end of solidification, which transforms almost completely to austenite in the solid state on cooling. In austenitic stainless steel weld metal the retention of ferrite, from a few percent to as high as 15–20%, is aided by two factors—the segregation pattern of Cr and Ni subsequent to solidification, and the rapid cooling rates prevailing during welding that prevent diffusion of Cr and Ni. A large volume of literature is devoted to the prediction and measurement of δ-ferrite in stainless steel weld metal. In predicting ferrite, the need for considering the effects of various alloying elements and non-equilibrium conditions prevailing during welding has given rise to the concept of chromium and nickel equivalents. The evolution of constitution diagrams for ferrite prediction has been reviewed by Olson (1985).

While considering cracking susceptibility, in addition to the room temperature ferrite content, information on the solidification mode is more relevant. Hammar & Svensson (1979) performed quenching experiments on a large number of alloys from the melting temperature to freeze the structure prevailing just after solidification. They developed the following equivalent formulae just for prediction of the solidification mode: $Cr_{eq} = Cr + 1{\cdot}37Mo + 1{\cdot}5Si + 2Nb + 3Ti$, and $Ni_{eq} = Ni + 0{\cdot}31Mn + 22C + 14{\cdot}2N + Cu$. According to this formula, the transition from AF to FA mode occurs at a Cr_{eq}/Ni_{eq} ratio of 1·55. Extensive work by Suutala & Moisio (1979) and Suutala (1983) showed that the above equivalents predict the solidification mode satisfactorily, based on which the solidification paths were determined for a large number of compositions.

With the increased use of duplex stainless steels, the DeLong diagram was found no longer adequate. Siewert *et al* (1988) proposed a new ferrite diagram that predicted ferrite up to 100 FN and thus covered the complete range of austenitic and duplex stainless steels. The diagram, shown in figure 4, is since known as the WRC-92 diagram (Kotecki & Siewert 1992). The accuracy of this diagram is superior to that of the DeLong diagram, since the bias due to a higher coefficient for N has been removed. More importantly from the point of view of cracking, the solidification mode boundaries have been included. Recent theoretical approaches to ferrite prediction using thermodynamic phase stability (Babu *et al* 1997) and using artificial neural networks (Vitek *et al* 2000) have led to greater improvements in accuracy of ferrite prediction over that offered by the WRC-92 diagram.

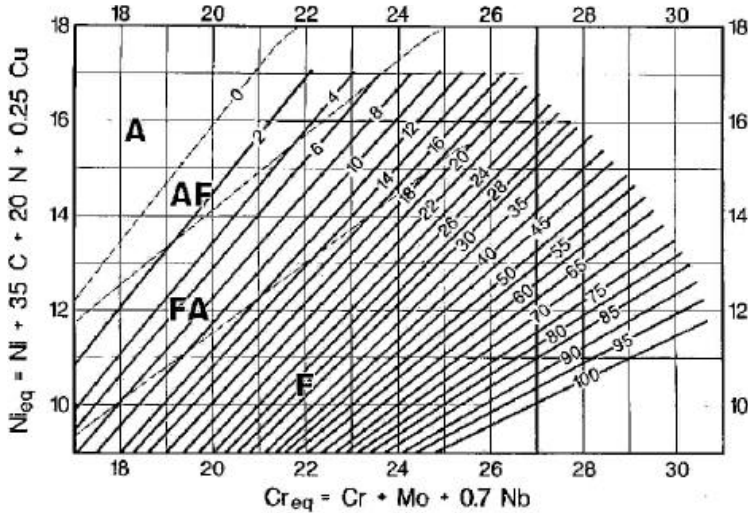

Figure 4. The WRC-92 constitution diagram for weld metal ferrite, including solidification mode boundaries.

2.2 *The relationship between solidification mode and room-temperature microstructure: The ferrite–austenite transformation*

The interpretation and analysis of weld microstructures in austenitic stainless steels is complicated by the superposition of the solid state transformation from ferrite to austenite over the as-solidified structure. The various ferrite morphologies observed at room temperature can be interpreted often only in terms of both the solidification mode and the subsequent solid state transformation. It is convenient to consider the change in composition in terms of Cr_{eq}/Ni_{eq} ratio. For low ratios, A-mode solidification occurs and there is no change in structure after solidification as no ferrite is present. For higher Cr_{eq}/Ni_{eq}, AF mode solidification occurs in which austenite is the primary phase and a part of the remaining liquid solidifies as intercellular ferrite. For higher Cr_{eq}/Ni_{eq} ratios during FA and F mode solidification, the high temperature microstructure has been shown to contain 70–100% ferrite (Thier 1987). On cooling to lower temperatures, most of the ferrite transforms and the residual ferrite left behind in the Cr-rich dendritic cores gives rise to the characteristic structure known as vermicular ferrite. Vermicular ferrite has been shown to result from a diffusional transformation at fairly high temperatures (1373–1573 K) under normal arc welding conditions (David *et al* 1979). For still higher Cr_{eq}/Ni_{eq} ratios in the FA and F modes, the ferrite is increasingly stable and the $\delta \rightarrow \delta + \gamma$ phase boundary occurs lower in temperature. At these lower transformation temperatures, an orientation relationship between the parent and product phases is favoured. As the transformation kinetics become sluggish, elongated acicular and Widmanstätten type morphologies are promoted.

3. The theory of hot cracking

Solidification cracking occurs predominantly by the segregation of solutes to form low-melting phases, which under the action of shrinkage stresses accompanying solidification cause cracking. Several theories have been advanced to explain the phenomenon (Pellini

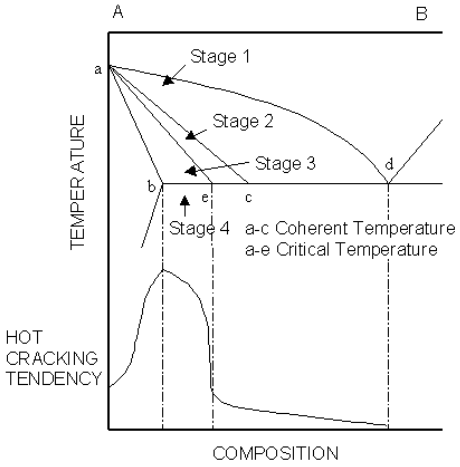

Figure 5. Effect of constitutional features on cracking susceptibility in binary systems according to the generalized theory of Borland (1960).

1952; Medovar 1954; Borland 1960; Holt 1992). The initial theories (Medovar 1954) took into account the fact that cracking is associated with segregation; the wider the liquid–solid range of the alloy, the greater the susceptibility. However, this theory was not entirely satisfactory, as several exceptions could be found and the freezing range appeared to be only one of many factors influencing cracking. The 'Generalised Theory' of cracking was proposed by Borland (1960). According to Borland, solidification involves four stages that are classified according to the distribution of the liquid and solid phases, as shown in figure 5 for a binary alloy. In stage 1, the solid phase is dispersed, the liquid phase is continuous and both the phases can accommodate relative movement. In stage 2, both liquid and solid phases are continuous, but the solid dendrites are interlocked and only the liquid is capable of movement. At this stage, the liquid can heal any cracks formed. In stage 3, the solid crystals are in an advanced stage of development and the free passage of liquid is prevented. The liquid is present in very small quantity. At this stage, if a stress is applied which exceeds the tolerance of the material, cracking can occur, which cannot be filled by the remaining liquid phase. This stage, during which much of the cracking occurs, is called the critical solidification range (CSR). In stage 4, solidification is complete and no cracking involving the liquid phase is possible.

Borland stated that for high cracking susceptibility, in addition to a wide freezing range, the liquid must also be distributed in a way that allows high stresses to be built up between grains. The extreme cases in which liquid can be distributed are as films or as isolated droplets, the actual behaviour depending on the interfacial energies of the solid and liquid phases. The angle of wetting of the solid interfaces by the liquid is related to the interfacial energies as follows (Smith 1948):

$$\gamma_{SL}/\gamma_{SS} = 1/(2\cos\theta/2) = \tau,$$

where γ_{SL} and γ_{SS} are the energies of the solid–liquid interface and the solid–solid grain boundary respectively and θ is the dihedral wetting angle, which varies between 0 and 180. Figure 6 shows the variation of θ with increasing interfacial energy ratio τ.

Wetting of the grain boundaries by a continuous liquid film occurs for τ less than $0{\cdot}5(\theta < 60)$ and for values above 0·5, the resistance to cracking increases. The higher the solid–liquid surface energy, the greater is the tendency to minimise the liquid–solid interface by formation of isolated pockets of liquid instead of continuous films. Borland showed that the interfacial energy ratio for iron–iron sulphide films was close to 0·5, explaining the deleterious effect

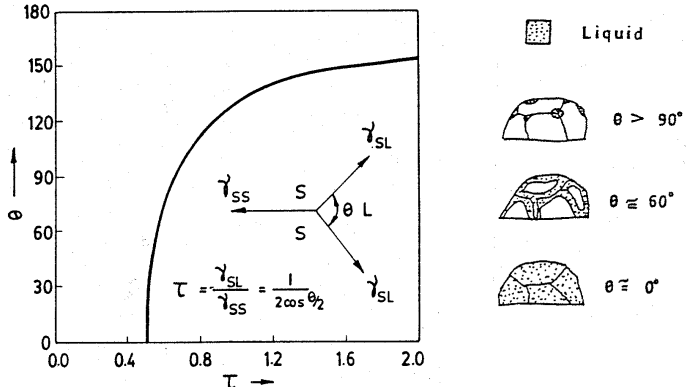

Figure 6. The variation of dihedral contact angle between liquid and solid phases with surface energy ratio; the change in grain wetting behaviour with decreasing wetting angle is also illustrated.

of sulphur in steels. The theory revealed the importance of wetting in relation to cracking. However, Borland's theory suffers from a few practical difficulties as listed below: (a) the non-equilibrium nature of the segregation would maximise the freezing range for even very dilute alloys, which the theory does not take into account (Clyne & Davies 1981), and (b) the effect of wetting angle of the liquid and solid phases on cracking is very difficult to quantify.

According to the generalised theory, hot cracks are believed to initiate during the later stages of solidification when most of the liquid has solidified. Some experimental observations (Matsuda *et al* 1982b; Semenyuk *et al* 1986) have shown, however, that hot cracks can initiate at temperatures very close to the liquidus and at much smaller fractions of solid than previously believed ($f_S \approx 0{\cdot}15$). In a recent review, Matsuda (1990) has suggested that crack initiation and propagation must be considered separately, and proposed a modification to Borland's theory. According to the modified theory, the critical solidification range (stage 3) starts at a higher temperature (closer to the liquidus) and is divided into two stages (figure 7), an initiation stage (stage 3(h)) where cracks can initiate and a propagation stage (stage 3(l)) where an already-existing crack grows. Many investigators believe (Borland 1960; Prokhorov & Prokhorov 1971) that there exists a temperature range during solidification over which

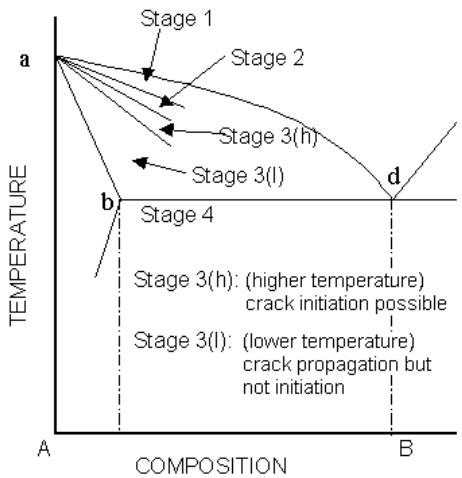

Figure 7. Modified concept of the effect of constitution on cracking susceptibility in binary systems (Matsuda 1990).

a material remains prone to brittleness that is measurable experimentally. The idea is that, irrespective of the stress field experienced during welding, the temperature range of susceptibility known as the brittle temperature range or BTR, can be considered a function of the composition.

Matsuda *et al* (1989a, b) have shown that the BTR can be obtained by calculation of liquid composition applying the Schiel equation and using suitable numerical techniques for computation. Hot cracking test methods that enable measurement of the brittleness temperature range (BTR) are therefore very useful in predicting cracking in actual situations. This is discussed further in a subsequent section.

4. Solidification cracking in austenitic stainless steel welds

4.1 *Forms of solidification cracking*

Solidification cracking is observed as (a) gross cracking, occurring at the junctions of dendrites with differing orientations, detectable by visual and liquid penetrant testing, and (b) microfissuring in the interdendritic regions which are revealed only by application of strain to the cracked region or at high magnifications. The increase in cracking that occurs when the solidification range is widened by the formation of low-melting eutectics with impurity elements was identified by early investigators and various theories of hot cracking were developed, as already discussed. Composition affects the tendency of stainless steel weld metal towards cracking in two major ways. First, as discussed earlier, the primary mode of solidification from the liquid is a function of composition and FA/F mode of solidification has been found to be beneficial in reducing cracking. Solidification mode determines the nature of the solid interfaces present during solidification. The second effect of composition is through segregation, which determines the wetting characteristics and constitutional supercooling in the interdendritic regions. The effects of solidification mode and composition on hot cracking will be discussed in detail in subsequent sections.

The heat input during welding also affects the hot cracking behaviour significantly, primarily by affecting the amount and scale of segregation. Goodwin (1988) using the Sigmajig test to evaluate GTAW, laser and electron beam welds found that increased heat inputs decreased the threshold stress for cracking, thereby increasing cracking susceptibility. Higher energy densities decreased cracking, and cracking resistance was progressively higher for GTAW, electron and laser beam welding, in the order of decreasing heat inputs. However, in arc welding of stainless steels where solidification rates do not vary over a wide range, differences in cracking attributable to welding parameter variations may not be significant.

4.2 *Effect of δ-ferrite and solidification mode on solidification cracking*

The effect of varying δ-ferrite contents on cracking in stainless steels was studied by Hull (1967) using the cast pin tear test. Hull found that, while the cracking susceptibility was high for fully austenitic compositions, specimens with 5–30% ferrite were quite resistant to cracking. When ferrite content increased further, the cracking sensitivity again increased. Masumoto *et al* (1972) found that it was the FA/F solidification mode that was essential to reducing cracking rather than residual ferrite content after welding. Subsequently, various investigations were conducted using hot cracking tests for different commercially used compositions. Kujanpaa *et al* (1979) represented cracking data from the literature on a map of $P + S$ vs. Cr_{eq}/Ni_{eq} ratio. They used the Schaeffler equivalent formulae for Cr and Ni to calculate the ratio. On this map, they plotted cracking data from a number of studies, including

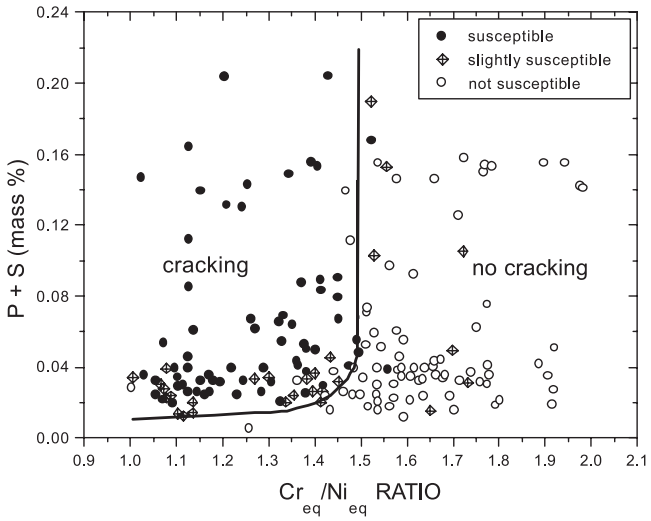

Figure 8. Solidification cracking behaviour in austenitic stainless steel welds as a function of Schaeffler Cr_{eq}/Ni_{eq} ratio and P+S levels (after Kujanpaa *et al* 1979).

their own, as shown in figure 8. They found that highly susceptible compositions lay bounded by a curve with a lower limit of 0·01–0·015 wt.% P + S, and limited on the Cr_{eq}/Ni_{eq} axis by a value of 1·5, up to which a primary austenitic solidification mode exists. Thus, compositions with Cr_{eq}/Ni_{eq} greater than 1·5 or with P + S < 0·01 wt% were 'not susceptible'. In effect, the diagram divided the compositions according to hot cracking susceptibility. However, the cracking propensity abruptly increased when the Cr_{eq}/Ni_{eq} ratio was below 1·5, unless the P + S content was below 0·01 wt%.

Lundin *et al* (1988c) modified this diagram to represent longitudinal varestraint test data on 3 mm thick specimens, which is shown in figure 9. The equivalent formulae used to calculate Cr_{eq}/Ni_{eq} ratio were changed to that of Hammar & Svensson (1979). Lundin classified the compositions on the basis of total crack length (TCL) in the varestraint test at 4% strain,

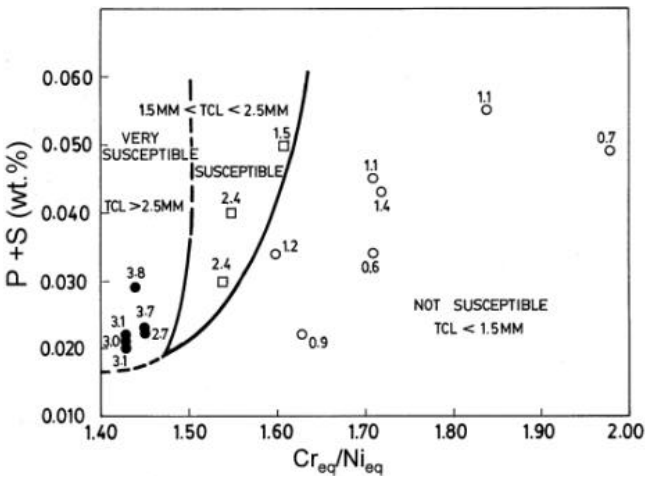

Figure 9. Solidification cracking behaviour in austenitic stainless steel welds as a function of Hammar–Svensson Cr_{eq}/Ni_{eq} ratio and P+S levels (Lundin *et al* 1988).

as 'highly susceptible' for TCL $>$ 2·5 mm, 'susceptible' for TCL between 1·5–2·5 mm, and 'not susceptible' for TCL $<$ 1·5 mm. When the data were plotted on this diagram, the mixed solidification mode FA region, in which Cr_{eq}/Ni_{eq} ratio is 1·5–1·6, was identified as having a cracking susceptibility intermediate between that of the A-mode and FA or F-mode materials. In this region, cracking was sensitive to P+S levels. The FA/F-mode materials with a Cr_{eq}/Ni_{eq} above 1·6 were quite tolerant to impurity elements even over 0·04 wt.%, while in A-mode materials ($Cr_{eq}/Ni_{eq} < 1.5$), cracking is high for P + S greater than about 0·015 wt.%.

A number of factors have been proposed to explain the beneficial effects of δ-ferrite on cracking behaviour:

(1) The higher solubility for impurity elements in δ-ferrite leads to less interdendritic segregation and reduces cracking tendency (Borland & Younger 1960).
(2) Cracks are arrested by the irregular path offered by a duplex austenite–ferrite structure. The peritectic/eutectic reaction interface arrests remaining pockets of liquid and thus crack propagation (Matsuda 1979).
(3) The lower surface energy of the γ–δ boundary and its reduced wettability by eutectic films compared to γ–γ or δ–δ interfaces is an important factor (Hull 1967).
(4) The presence of ferrite results in a larger interface area due to the solid state transformation to austenite that begins soon after solidification. The increased area disperses the concentration of impurity elements at the grain boundaries.
(5) The ductility of ferrite at high temperatures is greater than that of austenite, allowing relaxation of thermal stresses.
(6) The lower thermal expansion coefficient of ferrite as compared to austenite results in less contraction stresses and fissuring tendency.
(7) The solidification temperature range of primary ferrite welds is less than that of primary austenite solidified welds, providing a smaller critical temperature range for crack formation (Pellini 1952).
(8) The presence of ferrite refines the grain size of the solidified metal, which results in better mechanical properties and cracking resistance.
(9) The higher coefficients for impurity diffusion in ferrite as compared with austenite allow faster homogenisation in ferrite and less tendency for cracking.
(10) Coarse grain formation in the HAZ occurring by recrystallisation and grain growth in fully austenitic metals increases susceptibility to liquation cracking (Kujanpaa *et al* 1987), while ferrite forming compositions are not susceptible.
(11) The volume contraction associated with the ferrite-austenite transformation reduces tensile stresses close to the crack tip, which decreases cracking tendency (Thier *et al* 1987).

Brooks *et al* (1991) argue that since solidification cracking is associated mainly with grain boundaries, those factors that affect the nature of the grain boundaries should be more relevant to cracking behaviour. From this standpoint, a review of the literature suggests that the major factors that make FA/F mode weld metals resistant can be listed as, (a) the higher solubility of S, P etc., in the ferrite that introduces less of the harmful solute in the interdendritic regions, (b) lower wettability of grain boundaries in a duplex structure and (c) grain refinement during FA mode solidification. Hence the factors 1–4 and 8 listed above can be considered of major importance. Factors 5 and 6 relating to ductility and thermal expansion of ferrite appear less likely, since cracking is higher for the F-mode in relation to FA mode weld metals (Matsuda *et al* 1986, 1989b). The other factors may have a relatively minor but contributory role to

play. However, it must be mentioned that the mechanics of the cracking process is still not completely understood.

4.3 *Effects of impurity and alloy elements on cracking*

The bulk of the literature on hot cracking is devoted to the study of compositional effects due to impurities and minor elements. Hull (1960) in stainless steels and Borland & Younger (1960) in steels reviewed the influence of several elements on cracking sensitivity. Accordingly, sulphur, phosphorus, boron, niobium, titanium and silicon were identified as most harmful. These elements strongly partition to the liquid, possess low solubilities in solidified steel and form low-melting eutectics with iron, chromium or nickel as shown in table 1. The low eutectic temperatures show the extent to which the solidus temperature can be lowered by eutectic formation. The effects of the individual elements will be further considered.

Among the elements whose effects on cracking were investigated, Hull (1960) found molybdenum, manganese and nitrogen beneficial. Kakhovskii *et al* (1971) state that these elements increase the resistance of fully austenitic weld metal to cracking by retarding polygonisation. Presumably, these elements bind to the lattice defects during solidification and reduce the concentration of defects at the solidification subgrain boundaries, which decreases their wettability.

4.3a *Effects of sulphur and phosphorus:* Sulphur is known to be an undesirable impurity in welding of stainless steels due to the formation of low-melting sulphide films along the interdendritic and grain-boundary regions. Sulphur is almost insoluble in all three major constituents of stainless steel, viz. iron, chromium and nickel. The phase diagrams for sulphur binaries with all three elements show wide and deep solid–liquid regions with low partition

Table 1. Partition coefficients of elements promoting hot cracking in austenite and ferrite, constitution and melting points of possible low-melting phases. Data from Folkhard (1988) and Matsuda *et al* (1989).

	Temp.	Partition coeff.		Low-melting phases	
Constituent	(K)	δ	γ	Structure	m p (K)
Sulphur	1638	0·091	0·035	Eutectic Fe–FeS	1261
				Eutectic Ni–NiS	903
Phosphorus	1523	0·23	0·13	Eutectic Fe–Fe_3P	1321
				Eutectic Ni–Ni_3P	1148
Boron	1654	0·125	0·001	Eutectic Fe–Fe_2B	1450
				Eutectic Ni–Ni_2B	1413
				Eutectic $(Fe,Cr)_2B$-γ	1453
Niobium	1573	0·28	*	Eutectic Fe–Fe_2Nb	1643
				Eutectic NbC-γ	1588
				Nb–Ni rich phase	1433
Titanium	1573	0·57	*	Eutectic Fe–Fe_2Ti	1563
				Eutectic TiC-γ	1593
Silicon	1573	0·77	0·52	Eutectic Fe–Fe_2Si	1485
				Eutectic NiSi–Ni_3Si_2	1237
				NiSi-γ	1269

*Not known

coefficients for sulphur in austenite. Sulphur is strongly rejected into the liquid during solidification of austenite, rapidly lowering the melting point of the interdendritic liquid. Thus, the potential for forming low-melting eutectics remains strong even with very low contents in austenite ($< 0{\cdot}005$ wt.%) (Matsuda 1981). On the other hand, δ-ferrite shows higher solubility for elements like S, P, Si and Nb.

Solidification in the FA mode is known to increase tolerance for S content to as high as 0·05 wt.% without hot cracking. Lundin *et al* (1988a) investigated weldability of free-machining stainless steels, and found that, provided a ferritic solidification mode is maintained, steels with sulphur contents of up to 0·35 wt.% could show satisfactory weldability. However, in the case of type 310 steel solidifying in the austenitic mode, sulphide films were present even with 0·005 wt.% S and increased the brittleness temperature range along with phosphorus. Matsuda *et al* (1981) recommended that for fully austenitic stainless steels, the maximum S and P contents are 0·005 and 0·006 wt.% respectively, to avoid fusion zone cracking. In a study of heat-affected zone cracking in a titanium-containing 15Cr–15Ni steel, Persson (1971) and Egnell & May (1970) found grain-boundary precipitates of titanium carbosulphide or titanium sulphide which decreased the hot ductility in the temperature range 1373–1573 K. Kujanpaa *et al* (1987) found sulphur enrichment of 2000 times at HAZ cracks in type 310 stainless steel. Thus, the harmful role of sulphur in hot cracking is evident.

Phosphorus ranks next to sulphur in the list of elements detrimental to good weldability in stainless steels. Like sulphur, P forms low-melting eutectics with iron, chromium and nickel. The maximum solubility of P in austenite at the eutectic point (1423 K) with iron is 0·25 wt.% and that in ferrite is 2·8 wt.% at 1323 K. Phosphide eutectics at interdendritic regions have been found to extend the brittleness temperature range in varestraint testing to as much as 250 K lower than the solidus in fully austenitic type 310 steel (Matsuda *et al* 1981). The segregation tendency remains high due to the wide solid–liquid range and low eutectic temperatures (1373 K). Brooks (1974) identifies phosphorus as particularly harmful in fully austenitic stainless steels since it has a strong tendency to spread as liquid films. Further, it has been stated that the low diffusivity of P in both austenite and ferrite phases even at high temperatures virtually precludes homogenisation (Folkhard 1988).

The harmful effects of S and P have led to work on addition of other elements that counteract their effects. Manganese additions are well-known to decrease cracking in high-S steels by forming higher-melting MnS-γ eutectics in preference to FeS (Hull 1960; Dixon 1988). Further, the addition of lanthanum and other rare-earths has been found highly effective in binding the P and S as stable compounds (Matsuda *et al* 1982a).

4.3b *Nitrogen in austenitic stainless steel welds:* In 316LN stainless steel for nuclear service, carbon has been reduced to decrease the propensity for intergranular corrosion. Nitrogen is added mainly to recover the higher strength and elevated temperature properties associated with the loss of carbon in comparison with conventional 316 (Eckenrod & Kovach 1979). Nitrogen has potent effects on the microstructure and hence is expected to have strong influence on hot cracking behaviour also. The influence of nitrogen on hot cracking of austenitic stainless steel weld metal has been reviewed by Menon & Kotecki (1989). Nitrogen in weld metal arises from various sources such as prior content in the base metal, intentional addition through the shielding gas or as inadvertent pickup due to inadequate shielding during welding.

Nitrogen resides in weld metal in the following forms (Stevens 1989): (i) interstitial nitrogen dissolved in the lattice structure – may collect around lattice defects, (ii) combined nitrogen present as nitrides, and (iii) occluded nitrogen in pores. It is the first two forms of nitrogen that affect the metallurgical behaviour of the weld metal. According to Eckenrod & Kovach

(1979), 18-8 type stainless steels with nitrogen up to 0·16 wt.% N show very good weldability with no porosity or loss of nitrogen. However, with increased nitrogen to 0·24 wt.%, pinholes and porosity due to nitrogen evolution are observed.

Nitrogen has a strong stabilising effect on austenite when present in iron and Fe–N austenite is isomorphous with Fe–C austenite in the Fe–C–N system. The solubility of nitrogen in austenite is enhanced by several solutes such as Cr, Mn and to a greater extent by V and Nb. Mo increases solubility slightly while C, Si and Ni tend to decrease it (Pehlke & Elliott 1960). However, in commercial compositions containing several elements in combination, synergistic effects are present that make prediction of actual nitrogen pickup in weld metal difficult. The nitrogen activity in steel decreases when elements with high N-affinity such as Al, Cr, V, or Nb are added, while it increases with additions of C, Ni, P, S or Si (Stevens 1989).

During GTA welding, it has been shown that the weld nitrogen content does not follow Sievert's Law but is proportional to the nitrogen partial pressure in the shielding gas (Blake 1979). When welding with pure argon, a nitrogen pickup of 0·02–0·03 wt.% usually occurs, which is believed to result from imperfect shielding from the atmosphere. By deliberate addition of up to 20 vol.% nitrogen through the shielding gas, a maximum pickup of about 0·25 wt.% N has been reported in 304 and 316 type stainless steels (Arata *et al* 1974; Ogawa & Tsunetomi 1982; Lundin *et al* 1988a; Mudali *et al* 1986). The variation in N pickup reported in different studies for similar shielding gas compositions appears to be related to two factors, namely variations in composition of the weld metal and the oxygen content in the shielding atmosphere, both of which have major influence. Under identical conditions, Mudali *et al* (1986) reported that type 304 picks up more N than 316 for the same partial pressure of nitrogen, as shown in figure 10.

4.3c *Effects of nitrogen on solidification cracking:* In FA mode compositions, the most direct effect of nitrogen on cracking is through a decrease in weld metal ferrite content. Nitrogen, by stabilising the austenite phase, decreases the occurrence of primary δ-ferrite, which results in reduced resistance to cracking. Several studies that focused on the possible role of nitrogen in influencing hot cracking behaviour (Arata *et al* 1974; Cieslak *et al* 1982; Matsuda *et al* 1983a; Ogawa *et al* 1984) point to the fact that nitrogen changes the solidification mode from ferritic to austenitic, thus increasing the cracking. Matsuda *et al* (1983a) investigated cracking in type 304 weld metal with nitrogen addition. They concluded that nitrogen addition

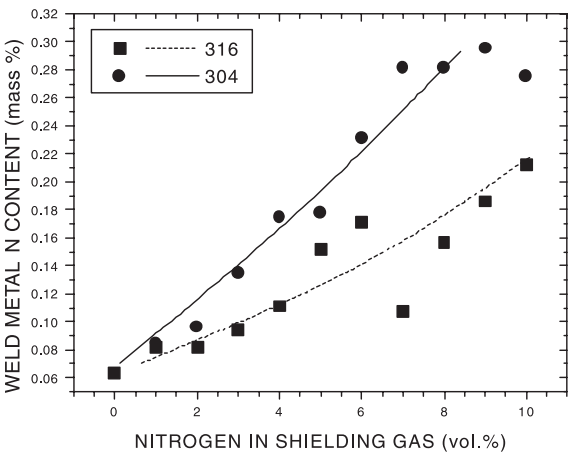

Figure 10. Nitrogen content obtained in weld metal as a function of nitrogen content in argon shielding gas for type 304 and 316 weld metals (data of Mudali *et al* 1986).

decreases the amount of primary ferrite, which also reduces the residual ferrite content. Their investigations also found increasing amounts of phosphides and sulphides at the grain boundaries with nitrogen addition, which promotes cracking. The cracking is characterised by the brittleness temperature range (BTR), which increases with nitrogen content to reach values similar to that of fully austenitic type 310. On the other hand, Lundin *et al* (1980) did not find any detrimental effect in their study on 316 weld metal with increasing nitrogen content, presumably because of the low impurity levels in the material. Zhitnikov (1981) reported that if the ferrite content is kept constant, increase in the nitrogen level is not detrimental to hot cracking resistance and may even have a slight beneficial effect. However, information on the levels of P and S in their materials is not available. In summary, it appears that the effect of nitrogen in weld metal containing ferrite (or ferritic solidification mode) is related to the levels of impurity elements. Hence nitrogen is probably detrimental in high-impurity weld metal ($> 0{\cdot}04$ wt.%), but may have a neutral or beneficial effect in relatively pure compositions.

In fully austenitic stainless steels, the effects of nitrogen on cracking have been investigated by several workers (Kakhovskii *et al* 1971; Arata *et al* 1974; Zhitnikov *et al* 1981; Ogawa & Tsunetomi 1982; Matsuda *et al* 1983a; Lundin *et al* 1988a). However, the findings are controversial and indicate the complex effect of nitrogen on weld metal solidification. Kakhovskii (1971) and Zhitnikov (1981) reported beneficial effects of nitrogen addition of up to 0·2 wt.% in 18Cr–14Ni type steel. Similar results were reported by Ogawa & Tsunetomi (1982) in type 310 stainless steel and for 316L by Lundin *et al* (1988c). The beneficial effects of nitrogen in these cases have been attributed to the retardation of polygonisation (Zhitnikov 1981) and to a refinement in the dendritic structure (Lundin *et al* 1988c). On the other hand, Arata *et al* (1974) found no significant effect of nitrogen contents up to 0·16 wt.% on cracking in type 310. Further, Brooks (1975) reported a detrimental effect of high nitrogen contents ($> 0{\cdot}4$ wt.%) on cracking in high-manganese 21-6-9 welds, probably by the formation of a nitrogen-rich M_6X type of eutectic. M_6X-type phases along with Cr_2N and Fe_4N have also been found in 17·5Cr–13Ni–2·8Mo weld metal with 0·13 to 0·24 wt.% N (Omsen & Eliasson 1971). However, no subsequent study has confirmed the existence of these phases. There is no strong evidence that N may either segregate strongly during solidification or form low-melting eutectics unlike C, which is known to form various carbide-based eutectics. Further, there has been no attempt to associate the effect of nitrogen and cracking with the levels of impurity elements. In recent work (Shankar 2000), N additions enhanced cracking in fully austenitic 316L weld metal with high S (0·012%) but did not increase cracking in low-S (0·001%) weld metal. The P levels in these steels are 0·035% and 0·031% respectively. It was concluded in this study that at high S levels, N acts synergistically with S to increase cracking.

In summary, it appears that nitrogen has diverse effects on the microstructure with corresponding consequences on the cracking behaviour of type 316 stainless steel.

(a) In FA mode alloys, a reduction in ferrite content and increase in segregation, leading to an increase in cracking.
(b) In A-mode alloys, retardation of polygonisation, which decreases wettability and hence cracking.
(c) In fully austenitic alloys, a refining effect on the solidification structure leading to a decrease in the cracking at moderate levels (up to 0·16 wt.%).
(d) N appears to act synergistically with S to increase cracking in fully austenitic 316L weld metal; low-S weld metal shows no effect on increasing N levels.

4.3d *Effects of titanium and niobium on cracking in stabilized stainless steels:* Austenitic stainless steels stabilized with titanium or niobium such as types 321 and 347 are known to exhibit higher susceptibility to hot cracking than the unstabilized varieties. Both these elements stabilise ferrite and restrict the austenite phase field (Massalski 1996). Lundin *et al* (1975) found that, all other residual levels being equal, the presence of niobium alone contributed to increasing fissuring in type 347 weld metal and a ferrite number of 6 was required to completely eliminate fissuring. Arata *et al* (1974) found good weldability for type 321 and 347 steels only with high ferrite contents (6 FN or greater). Hence the problem of cracking is severe in such steels when the ferrite level is low, for instance, when ferrite is not desirable during service. In a study on the effects of various elements on cracking of fully austenitic type 347 stainless steel, Hoerl & Moore (1957) derived a statistical relation between composition and cracking using the segmented circular groove test. They found that increasing C and Mn has strong positive effects in decreasing cracking, while phosphorus, sulphur and silicon enhance cracking.

Phases responsible for cracking in stabilized stainless steels have been identified by several investigators. In alloy 800, Wolstenholme (1973) found that a eutectic of the type (Ti,Nb)C-γ is responsible for cracking, which was also confirmed by Lippold (1983). Matsuda *et al* (1983b) found that Ti addition up to 0·05 wt.% decreases the hot cracking tendency by increasing the melting point of low-melting phosphide eutectics. However, higher amounts to 0·6 wt.% increases the BTR during varestraint testing by up to 100 K. They found enrichment of P along with Ti in the low-melting constituents. Recent work by Shankar *et al* (2000) found titanium carbosulphides, carbonitride and carbide in solidification cracks in a 15Cr–15Ni–2Mo stainless steel with 0·2–0·4% Ti. Enrichment of C, N, S and Ti was detected using EPMA while phase identification was performed by X-ray diffraction analysis. Cracking increases with increasing Ti and is related to the amount of C + N present. The results suggest that cracking could be minimized by reducing the Ti/(C + N) to below a value of 3. Particularly significant is the enhancement of cracking caused by nitrogen pickup of $\sim$ 200 ppm during the welding process.

In Nb-containing type 310 stainless steel, Ogawa & Tsunetomi (1982) found considerable quantities of Nb(C,N) in the form of eutectic structures. Lundin *et al* (1988a) also found Nb(C,N)-austenite eutectic in fully austenitic type 347 steel and further reported that increase in the ratio Nb/2(30C + 50N) increases cracking susceptibility. In an interesting study, Jolley & Geraghty (1979) found that in 18Cr–13Ni–1Nb steel, the high spreading tendency of niobium-containing eutectics is neutralised by the addition of 0·25 wt.% magnesium. Magnesium addition appeares to globularise the harmful eutectic phase. However, there are no further reports on whether magnesium additions are otherwise desirable.

It is clear that both Ti and Nb interact strongly with minor alloying elements such as C and N and impurities such as P and S. Hence the cracking susceptibility of stabilized stainless steels is influenced strongly by the stabilisation ratio, particularly the C and N levels in relation to the Ti and Nb and the levels of impurity elements.

5. Evaluation of hot cracking in austenitic stainless steel weldments

5.1 *Hot cracking evaluation criteria*

Hot cracking is believed to occur owing the inability of the solidifying weld metal to support strain in a critical temperature range during freezing (Borland 1960). The cracking is a function of composition as well as strain. In actual welds, the amount of strain experienced by the weld

metal is difficult to estimate in view of complex geometric and thermal conditions. Hence controlled strain applied on a geometrically simple specimen is preferred for evaluation of cracking tendency. Several tests exist that satisfy the above condition, such as the varestraint test, the PVR test (programmierter Verformungsrisstest) and the sigmajig test.

The varestraint test (Savage & Lundin 1965) uses a controlled, rapidly applied bending strain to produce cracking, and crack lengths are used for evaluation. In the PVR test (Rabensteiner *et al* 1983), the tensile strain rate is increased during welding and the critical strain rate for onset of cracking is measured, while in the sigmajig test (Goodwin 1987), the critical tensile stress for crack initiation is determined. The longitudinal varestraint test and the related Transvarestraint test are more widely used for assessment of hot cracking during welding than the other two tests (Goodwin 1990). In the longitudinal varestraint test (LVT) strain is applied in the direction of welding, whereas in the transvarestraint test (TVT), it is applied transverse to the welding direction. In the LVT, the total crack length (TCL) and cracking threshold strain are considered the most important assessment criteria (Lundin *et al* 1982), while in the TVT the maximum crack length (MCL) is used for assessment. In addition, in the TVT, the MCL is used for estimating the temperature range of cracking during solidification called the brittleness temperature range or BTR. Many studies have focused on determination of BTR, which is possible using the varestraint type of test.

The procedure for calculating BTR from MCL is shown schematically in figure 11. To calculate BTR, the cooling curve at the centreline of the weld is obtained by plunging a thermocouple behind the arc. The temperature-time variation of the cooling curve can be converted into a temperature-distance relation using the transformation *distance = speed x time*. This is shown schematically in figure 11, which gives the temperature profile around the weld puddle at the instant of strain application. The crack length is mapped on to this temperature field as a function of distance from the molten zone. The difference between the temperatures at either end of the longest crack then gives the brittleness temperature range (BTR). The MCL can thus be used to determine BTR. The starting temperature for BTR is assumed to be at the intersection of molten and solid state cooling curves. The temperature associated with a distance corresponding to MCL gives the lower temperature of the BTR.

While the temperature range of cracking is the major component of cracking susceptibility, strain is an essential condition to produce cracking. The BTR can therefore be expressed

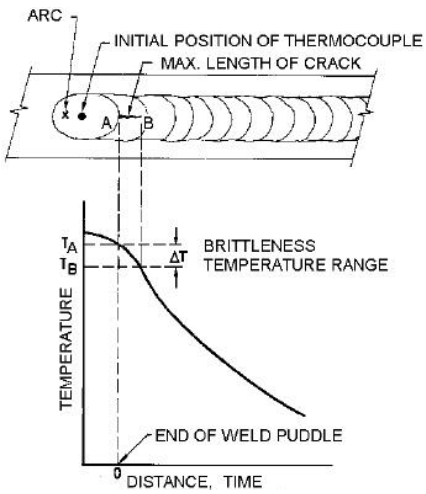

Figure 11. Procedure for calculating BTR from the MCL and weld centreline cooling curve (after Lundin & Savage 1965).

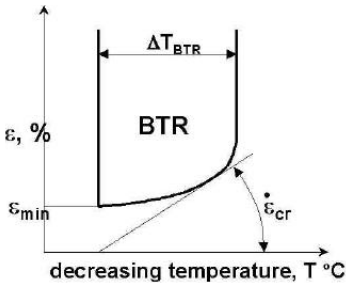

Figure 12. The concept of brittleness temperature range (BTR) during solidification of metals in the strain-temperature regime (after Prokhorov & Prokhorov 1971).

as a region in temperature-strain space, as shown in figure 12. This figure shows that the cracking continues down to a lower temperature as strain is increased and that it saturates at a certain minimum temperature. In many materials a minimum strain $\varepsilon_{\min}$ is required to initiate cracking called the cracking threshold and also a critical strain rate $\dot{\varepsilon}_{\rm cr}$ for cracking to occur, as shown in the figure. Various tests for hot cracking are designed to measure one or more of these quantities. In the TVT, the BTR is determined in terms of strain, since the MCL can be derived as a function of strain. In the PVR test, the critical strain rate for cracking is measured.

One advantage of the LVT is that in addition to fusion zone cracking, HAZ cracking can also be studied in the same specimen, which is not possible using TVT. It is interesting to consider the question of estimating BTR using the LVT. When the varestraint test was originally developed, it was claimed that the BTR could also be determined from this test. However, in the longitudinal varestraint test, the longest cracks are rarely found at the weld centreline where segregation is highest. In the transvarestraint test (TVT) on the other hand, the weld is strained transverse to the welding direction, which always produces cracking close to the weld centreline. Hence the TVT is widely preferred for determination of BTR (Arata *et al* 1974). Much work has been done using the Transvarestraint test in Japan, to evaluate the brittleness temperature range (Arata *et al* 1977). It is widely believed that TVT is superior to other methods of testing for fusion zone hot cracking, because this test produces cracking along the weld centreline in almost all cases. Further, the MCL remains constant with strain, providing a true measure of metallurgical susceptibility. On the other hand in the LVT, MCL continues to increase with strain. Arata *et al* (1974) carried out both types of tests in several stainless steels and concluded that at high strains ($> 2{\cdot}5$ wt.%), the MCL values obtained by either method are equivalent. More recently, Lin *et al* (1992) have suggested that in the LVT, the actual distance between the isotherms at either end of the crack must be considered rather than the maximum crack length, for cracks that are away from the weld centreline. They proposed that this measure, termed maximum crack distance or MCD, is more relevant for BTR evaluation. Shankar *et al* (2000b) comparing results of the two tests showed that MCL from the LVT is always higher than that in the TVT. They found that MCD values from the LVT for ten different stainless steels were in direct proportion to the MCL from the TVT. The relation between MCD and MCL is shown in figure 13, which demonstrates that it is possible to reliably estimate BTR from the LVT.

5.2 *Relation between test criteria and actual cracking behaviour*

Although it is possible to assess materials for their relative susceptibility to cracking using the TCL and BTR criteria, application of these results to practical welding situations is complicated by the fact that in the actual case, strain, strain rate and stress are all variable even within a given geometrical configuration. Tests such as the Y-groove test (Miura 1981) or the

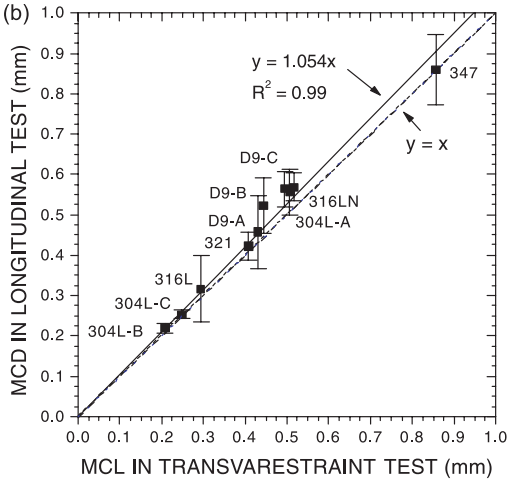

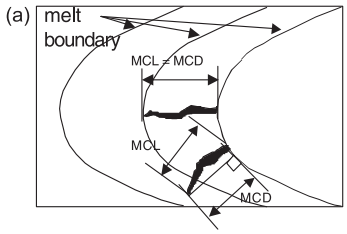

Figure 13. The concept of maximum crack distance (MCD) in the LVT and its relation to the MCL in transvarestraint test, **(a)** relation between MCD and MCL for centreline cracks and off-centreline cracks and **(b)** Correlation between MCD in longitudinal test and MCL in transvarestraint test at 4% strain.

circular patch test (Lingenfelter 1972) or actual weld joints have been used for correlation with varestraint test results. Lingenfelter found that the cracking behaviour of two heats of alloy 800, when welded by GTAW to form butt joints in 12 mm thickness, showed cracking as predicted by the varestraint test. Miura (1981) found good correlation between varestraint test results and cracking in the Y-groove test. He investigated several heats of 304, 316 and 347 stainless steels using the varestraint test as well as the Y-groove test. The cracked length in the Y-groove test specimens increases linearly with TCL in the varestraint test, after an initial threshold TCL value. Below this threshold TCL, there is no cracking in the Y-groove test.

However, Lin *et al* (1992) found that, when comparing cracking in pipe welds of two fully austenitic stainless steels, ranking based on BTR gives more accurate prediction of actual behaviour than TCL from the varestraint test. Recent work (Shankar 2000) has shown that weld bead geometry can have a significant effect on TCL. Changes in weld width, for example, can occur due to variations in levels of surface active elements such as S, O and to a lesser extent, N (Mills & Keene 1990). The TCL, when normalised by the weld width, shows good correlation with BTR, as shown in figure 14. Nevertheless, the study showed that the TCL is a complex parameter that depends on several factors apart from segregation leading to observation of a BTR such as the dendrite arm spacing, macroscopic grain structure, rheology of fluid flow, among others.

This literature review shows that opinion is divided on the choice of criteria for cracking assessment of materials. Further, there are difficulties in applying the results of variable restraint tests to actual welding situations. Recent work on hot cracking of low carbon steel during continuous casting (Won *et al* 2000) has shown that it is possible to get reliable predictions of cracking by taking into account the deformation of the solidifying metal, in addition to segregation effects. A similar approach in treating weld cracking could lead to better predictability of cracking behaviour.

6. Summary and conclusions

A review of solidification cracking in austenitic stainless steel welds shows that the problem is more prevalent in fully austenitic and stabilized stainless steels. Solidification mode is a major determinant of cracking susceptibility; ensuring an FA or F mode ensures the best resistance

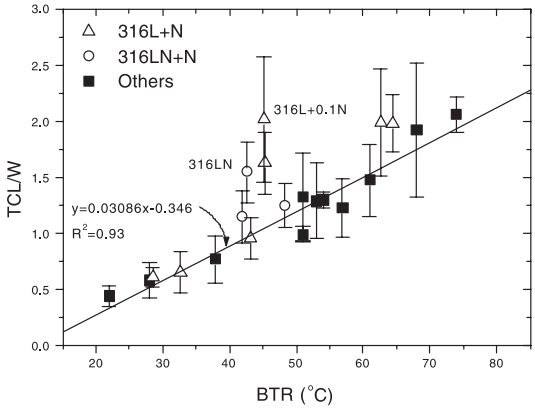

Figure 14. Correlation between TCL in longitudinal varestraint test and BTR (R^2 is the correlation coefficient and the equation shown is an error-weighted fit).

to cracking. The WRC-92 diagram has been found useful in determining safe compositional regimes for cracking based on the solidification mode criteria. Cracking is greater in more alloyed stainless steels than in leaner versions. In the latter the amount of retained ferrite is lower in the FA/F solidification modes than in the higher-alloyed steels.

A large number of studies have been done on the effect of impurity and alloying elements on cracking behaviour. The review considered in detail the effects of impurity elements S and P and alloying elements N, Ti and Nb on cracking. In N-enhanced stainless steels (N up to 0·2%), cracking is found to be dependent on the levels of impurity elements. Particularly S may have a synergistic detrimental effect when present at high levels in fully austenitic steels. There is no strong evidence that N may itself form low-melting phases unlike C, which is known to form various carbide-based eutectics. Ti and Nb increase cracking by forming various eutectics in conjunction with S, N and C. The most deleterious phases in such steels are probably the carbosulphides such as those of titanium, followed by the carbonitrides and the carbides. In Ti-bearing stainless steels, the amount of these phases increases with increasing stabilization ratio, i.e. (Ti,Nb)/(C,N). A lower ratio is desirable for minimizing the cracking propensity. In Ti-bearing fully austentic stainless steel Ti/(C+N) between 2 and 3 was found optimal.

Present theories on hot cracking suggest that cracking in welds depend on mechanical and metallurgical factors that are assumed to be independent of one another. However, there is controversy regarding at what stage during solidification cracking initiates. Some studies have shown that cracking could initiate very early during solidification (0·15 fraction solid). Recent work shows that prediction of cracking is more successful when mechanical behaviour of the solid is also considered than when only segregation is taken into account.

A review of hot cracking assessment methods and criteria shows that the brittleness temperature range or BTR is a useful concept. The BTR is determined from the maximum crack length in the varestraint test. An alternative way to measure cracking is to use a variable strain rate test to determine the critical strain rate for cracking. The BTR is much less subject to experimental variation than total crack length or TCL; one way to improve the reliability of TCL is to normalize crack length by weld width. Although impurity segregation is a major contributor to TCL, other factors such as dendrite arm spacing and grain orientations, also appear to have a minor role in determining TCL. Application of hot cracking test results to actual welding situations is complicated by the fact that the way strain is applied also influences cracking.

The authors are grateful to Dr. Baldev Raj for his keen interest and encouragement during the course of this work.

References

Arata Y, Matsuda F, Katayama S 1977 Solidification crack susceptibility in weld metals of fully austenitic stainless steels (report II) – effect of ferrite, P, S, C, Si, and Mn on ductility properties of solidification brittleness. *Trans. Jpn. Weld. Res. Inst.* 6: 105–116

Arata Y, Matsuda F, Saruwatari S 1974 Varestraint test for solidification crack susceptibility in weld metals of austenitic stainless steels. *Trans. Jpn. Weld. Res. Inst.* 3: 79–88

Babu S S, Vitek J M, Iskander Y S, David S A 1997 New model for prediction of ferrite number of stainless steel welds. *Sci. Technol. Welding Joining* 2: 279–285

Bhadeshia H K D H, David S A, Vitek J M 1991 Solidification sequences in stainless steel dissimilar alloy welds. *Mater. Sci. Technol.* 7: 50–61

Blake P D 1979 Nitrogen in steel weld metals. *Metal Constr.* 9: 196–197

Borland J C 1960 Generalized theory of super-solidus cracking in welds (and castings). *Br. Weld. J.* 7: 508–512

Borland J C, Younger R N 1960 Some aspects of cracking in welded Cr–Ni austenitic steels. *Br. Weld. J.* 7: 22–59

Brooks J A 1974 Effect of alloy modifications on HAZ cracking of A-286 stainless steel. *Weld. J.* 53: 517s–523s

Brooks J A 1975 Weldability of high N, high-Mn austenitic stainless steel. *Weld. J.* 54: 189s–195s

Brooks J A, Lambert Jr. F J 1978 The effects of phosphorus, sulfur and ferrite content on weld cracking of type 309 stainless steel. *Weld. J.* 57: 139s–143s

Brooks J A, Thompson A W, Williams J C 1984 A fundamental study of the beneficial effects of δ-ferrite in reducing weld cracking. *Weld. J.* 63: 71s–83s

Brooks J A, Thompson A W 1991 Microstructural development and solidification cracking susceptibility of austenitic stainless steel welds. *Int. Mater. Rev.* 36: 16–44

Cieslak M J, Ritter A M, Savage W F 1982 Solidification cracking and analytical electron microscopy of austenitic stainless steel weld metals. *Weld. J.* 61: 1s–8s

Clyne T W, Davies G J 1981 The influence of composition on solidification cracking susceptibility in binary alloy systems. *Bri. Foundryman* 74: 65–73

David S A, Goodwin G M, Braski D N 1979 Solidification behaviour of austenitic stainless steel filler metals. *Weld. J.* 58: 330s–336s

Dixon B 1988 Weld metal solidification cracking in austenitic stainless steels. *Aust. Weld. J.* 16: 2–10

Eckenrod J J, Kovach C W 1979 *Effect of nitrogen on the sensitization, corrosion and mechanical properties of 18Cr-8Ni stainless steels* (eds) C R Brinkman, H W Garvin, *ASTM STP* 679, pp 17–41

Egnell L, May W M 1970 Welding trials on a titanium-bearing austenitic steel. *Welding Inst. Conf. on welding of creep-resistant steels*, pp 144–151

Folkhard E 1988 *Welding metallurgy of stainless steels* (New York: Springer Verlag)

Fredriksson H 1979 Transition from peritectic to eutectic reaction in iron-base alloys. *Solidification and casting of metals* (London: The Metals Society) pp 131–138

Goodwin G M 1987 Development of a new hot-cracking test – the sigmajig. *Weld. J.* 66: 33s–38s

Goodwin G M 1988 The effects of heat input and weld process on hot cracking in stainless steel. *Weld. J.* 67: 88s–94s

Goodwin G M 1990 Test methods for evaluating hot cracking : review and perspective. *Advances in welding metallurgy* (Miami, FL: Am. Welding Soc./Jap. Welding Soc./Japn. Welding Eng. Soc.) pp 37–49

Hammar O, Svensson U 1979 Influence of steel composition on segregation and microstructure during solidification of austenitic stainless steels. *Solidification and casting of metals* (London: The Metals Society) pp 401–410

Hemsworth B, Boniszewski T, Eaton N F 1969 Classification and definition of high temperature welding cracks in alloys. *Met. Constr. Br. Weld. J.* 2: 5–16

Hoerl A, Moore T J 1957 The welding of type 347 steels. *Weld. J.* 46: 442s–448s

Hull F C 1960 Effects of alloying additions on hot cracking of austenitic stainless steels. *Proc. ASTM* 60: 667–690

Hull F C 1967 The effect of δ-ferrite on the hot cracking of stainless steel. *Weld. J.* 46: 399s–409s

Jolley G, Geraghty J E 1979 Solidification cracking in 18Cr–13Ni–1Nb stainless steel weld metal: the role of magnesium additions. *Solidification and casting of metals* (London: The Metals Society) pp 411–415

Kakhovskii N I *et al* 1971 Effects of silicon, nitrogen and manganese on chemical heterogeneity in type 0Kh23N28M3D3T weld metals and their resistance to hot cracking. *Avtomatich. Svarka* 8: 11–14

Kelly T F, Cohen M, Vandersande J B 1984 Rapid solidification of a droplet-processed stainless steel. *Met. Trans.* A15: 819–833

Koseki T, Flemings M C 1996 Solidification of undercooled Fe–Cr–Ni alloys part II – microstructural evolution. *Metall. Mater. Trans.* A27: 3226–3240

Koseki T, Matsumiya T, Yamada W, Ogawa T 1994 Numerical modeling of solidification and subsequent transformation of Fe–Cr–Ni alloys. *Metall. Mater. Trans.* A25: 1309–1321

Kotecki D J, Siewert T A 1992 WRC-1992 constitution diagram for stainless steel weld metals: A modification of the WRC-1988 diagram. *Weld. J.* 71: 171s–178s

Kujanpaa V, Suutala N, Takalo T, Moisio T 1979 Correlation between solidification cracking and microstructure in austenitic–ferritic stainless steel welds. *Weld. Res. Int.* 9: 55–76

Kujanpaa V P 1985 Effects of steel type and impurities in solidification cracking of austenenitic stainless steel welds. *Met. Constr.* 117: 40R–46R

Kurz W, Fischer D J 1985 *Fundamentals of solidification* (New York: Trans. Tech.)

Li L, Messler R W 1999 The effects of phosphorus and sulfur on susceptibility to weld hot cracking in austenitic stainless steels. *Weld. J.* 88: 387-s–396-s

Lin W, Nelson T, Lippold J C 1992 In *Proc. 'Eighth Annual North American Welding Research Conference'* (Columbus, OH: Am. Welding Soc./Edison Welding Inst./TWI) pp 1–6

Lingenfelter A C 1972 Varestraint testing of nickel alloys. *Weld. J.* 51: 430s–436s.

Lundin C D, DeLong W T, Spond D F 1975 Ferrite-fissuring relationships in austenitic stainless steel weld metals. *Weld. J.* 54: 241s–246s

Lundin C D, Chou C-P D, Sullivan D J 1980 Hot cracking resistance of austenitic stainless steel weld metals. *Weld. J.* 59: 226s–232s

Lundin C D, Lingenfelter A C, Grotke G E, Lessman G G, Matthews S J 1982 The varestraint test. *Weld. Res. Bull.* (280): 1–19

Lundin C D, Chou C-P D 1983 Hot cracking of austenitic stainless steels weld metals. *WRC Bull.* No. 289

Lundin C D, Menon R, Lee C H, Osorio V 1986 New concepts in varestraint testing for hot cracking. In *Welding Research: The State of the Art*, JDC University Research Symposium Proceedings, ASM, pp 33–42

Lundin C D, Lee C H, Menon R, Osorio V 1988a Weldability evaluations of modified 316 and 347 austenitic stainless steels: Part I – preliminary results. *Weld. J.* 67: 35s–46s

Lundin C D, Lee C H, Menon R 1988b Hot ductility and weldability of free machining austenitic stainless steel. *Weld. J.* 67: 119s–130s

Lundin C D, Lee C H, Qiao C Y P 1988c *Group sponsored study – weldability and hot ductility behaviour of nuclear grade austenitic stainless steels*. Final Report, Univ. of Tennessee, Knoxville, TN

Massalski T B 1996 *Alloy phase diagrams* (Metals Park, OH: ASM)

Masumoto I, Takami K, Kutsuna M 1972 Hot cracking of austenitic stainless steel weld metal. *J. Jpn. Welding Soc.* 41: 1306–1314

Matsuda F 1990 Hot crack susceptibility of weld metal. In *Advances in welding metallurgy* (Miami, FL: Am. Welding Soc./Jap. Welding Soc./Japn. Welding Eng. Soc.) pp 19–35

Matsuda F, Nakagawa H, Nakara K, Sasaki I 1976 *Trans. Jpn. Weld. Res. Inst.* 5: 53–67

Matsuda F, Nakagawa H, Uehara T, Katayama S, Arata Y 1979 A new explanation for role of δ-ferrite improving weld solidification crack susceptibility in austenitic stainless steel. *Trans. Jpn. Weld. Res. Inst.* 8: 105–112

Matsuda F, Katayama S, Arata Y 1981 Solidification crack susceptibility in weld metals of fully austenitic stainless steels – solidification crack susceptibility and amount of phosphide and sulphide in SUS 310 weld metal. *Trans. Jpn. Weld. Res. Inst.* 10: 201–212

Matsuda F, Nakagawa H, Katayama S, Arata Y 1982a Solidification crack susceptibility in weld metals of fully austenitic stainless steels (report VI) – effect of La or REM addition on solidification crack resistance. *Trans. Jpn. Weld. Res. Inst.* 11: 79–94

Matsuda F, Nakagawa H, Sorada K 1982b Dynamic observation of solidification and solidification cracking during welding with optical microscope. *Trans. Jpn. Weld. Res. Inst.* 11: 67–77

Matsuda F, Nakagawa H, Katayama S, Arata Y 1983a Solidification crack susceptibility in weld metals of fully austenitic stainless steels (report VIII) – effect of nitrogen on cracking in SUS 304 weld metal. *Trans. Jpn. Weld. Res. Inst.* 12: 89–95

Matsuda F, Katayama S, Arata Y 1983b Solidification crack susceptibility in weld metals of fully austenitic stainless steels (report IX) – effect of titanium on solidification crack resistance. *Trans. Jpn. Weld. Res. Inst.* 12: 87–92

Matsuda F, Nakagawa H, Kato I, Murata Y 1986 *Trans. Jpn. Weld. Res. Inst.* 15: 99–112

Matsuda F, Nakagawa H, Lee J B 1989a Weld cracking in duplex stainless steel (Report II) – modelling of cellular dendritic growth during weld solidification. *Trans. Jpn. Weld. Res. Inst.* 18: 107–117

Matsuda F, Nakagawa H, Lee J B 1989b Weld cracking in duplex stainless steel (Report III) – numerical analysis of solidification BTR in stainless steel. *Trans. Jpn. Weld. Res. Inst.* 18: 119–126

Maziasz P J 1989 Developing an austenitic stainless steel for improved performance in advanced fossil power facilities. *J. Met.* 12: 14–20

Medovar I 1954 On the nature of weld hot cracking. *Avtomatich. Svarka* 7: 12–28

Menon R, Kotecki D J 1989 Literature review – nitrogen in stainless steel weld metal. *WRC Bull.* No. 389, pp 142–161

Mills K C, Keene B J 1990 *Int. Mater. Rev.* 35: 185–216

Miura M 1981 Weldability of austenitic stainless steel tubes. *J. Sumitomo Met.* 34: 201–213

Mudali U K, Dayal R K, Gill T P S, Gnanamoorthy J B 1986 Influence of nitrogen addition on microstructure and pitting corrosion resistance of austenitic weld metals. *Werkstoffe Korros.* 37: 637–643

Ogawa T, Tsunetomi E 1982 Hot cracking susceptibility of austenitic stainless steels. *Weld. J.* 61: 82s–93s

Ogawa T, Suzuki K, Zaizen T 1984 The weldability of nitrogen-containing austenitic stainless steel: part II – porosity, cracking and creep properties. *Weld. J.* 63: 213s–223s

Olson D L 1985 Prediction of austenitic weld metal microstructure and properties. *Weld. J.* 64: 281s–295s

Omsen A, Eliasson L 1971 Distribution of nitrogen during solidification of a 17·5Cr–13Ni–2·8Mo stainless steel. *J. Iron Steel Inst.* 10: 830–833

Pehlke R D, Elliott J F 1960 *Trans. AIME* 218: 1088–1101

Pellini W S 1952 Strain theory of hot tearing. *Foundry* November 1952, p 125

Pepe J J, Savage W F 1967 Effects of constitutional liquation on 18-Ni maraging steel weldments. *Weld. J.* 46: 411s–422s

Persson N G 1971 The influence of sulphur on the structure and weldability of a titanium-bearing austenitic stainless steel. *Proc. of the Soviet-Swedish Symposium. Clean Steel*, Sandviken, Sweden I: 142–151

Prokhorov N N, Prokhorov N Nikol 1971 Fundamentals of the theory for technological strength of metals while crystallizing during welding. *Trans Jap. Welding Soc.* 2: 109–117

Rabensteiner G, Tosch J, Schaberiter H 1983 Hot cracking problems in different fully austenitic weld metals. *Weld. J.* 62: 21s–27s

Savage W F, Lundin C D 1965 Application of the varestraint technique to the study of weldability. *Weld. J.* 45: 497s–503s

Schaeffler A L 1949 Constitution diagram for stainless steel weld metal. *Met. Progr.* 56: 680–680B

Scherer R, Riedrich G, Hougardy H 1941 US Patent 2 240 672

Semenyuk N I, Rabkin D M, Korshun A O 1986 Determining the hot cracking temperature range in the welding of aluminium alloys. *Autom. Weld.* 39: 16–18

Shankar V 2000 *Role of compositional factors in hot cracking of austenitic stainless steel weldments*. PhD thesis, Indian Institute of Technology – Madras, Chennai

Shankar V, Gill T P S, Terrance A L E, Mannan S L, Sundaresan S 2000a Relation between microstructure, composition and hot cracking in Ti-stabilised austenitic stainless steel weldments. *Metall. Mater. Trans.* A31: 3109–3122

Shankar V, Gill T P S, Mannan S L, Sundaresan S 2000b Criteria for hot cracking evaluation in austenitic stainless steel welds using the longitudinal varestraint and transvarestraint tests. *Sci. Technol. Weld. Join.* 5: 91–97

Siewert T A, McCowan C N, Olson D L 1988 Ferrite number prediction to 100 FN in stainless steel weld metal. *Weld. J.* 37: 289s–298s

Smith C S 1948 Grains, phases and interfaces: an interpretation of microstructure. *Trans. Am. Inst. Mining Metall. Eng.* 175: 15–51

Stevens S M 1989 Forms of nitrogen in weld metal. *WRC Bull.* (369): pp 1–2

Suutala N, Moisio T 1979 *Solidification technology in the foundry and the casthouse* (London: The Metals Society)

Suutala N 1982 Effect of manganese and nitrogen on the solidification mode in austenitic stainless steel welds. *Met. Trans.* A13: 2121–2130

Suutala N 1983 Effect of solidification conditions on the solidification mode in austenitic stainless steels. *Met. Trans.* A14: 191–197

Thier H, Killing R, Killing U 1987 Solidification modes of weldments in corrosion resistant steels – how to make them visible. *Met. Constr.* 19: 127–130

Vitek J M, Iskander Y S, Oblow E M 2000 Improved ferrite number prediction in stainless steel arc welds using artificial neural networks – Parts I and II. *Weld. J.* 79: 33-s–40-s, 41-s–50-s

Won Y M, Yeo T-J, Seol D J, Oh K H 2000 A new criterion for internal crack formation in continuously cast steels. *Met. Mater. Trans.* B31: 779–794

Wolstenholme D A 1973 Weld crater cracking in Incoloy 800. *Weld. Met. Fabrication* 41: 433–438

Zhitnikov N P 1981 The hot cracking resistance of austenitic CrNi weld metal and weld zone in relation to nitrogen content. *Weld. Prod.* 3: 14–16